Progress In Electromagnetics Research C, Vol. 118, 125–134, 2022

Design and Fabrication of COVID-19 Microstrip Patch Antenna for Wireless Applications

Jihan S. Abdaljabar[1, *], Mervat Madi[2], Asaad Alhindawi[3], and Karim Kabalan[4]

Abstract—This paper presents a novel unique microstrip fractal patch antenna with a COVID-19 shape designed for wireless applications. The COVID-19 antenna is a compact, miniature size, multiband, low weight, and low-cost patch antenna; the demonstrated patch antenna, simulated using the HFSS software program, consists of a circular printed patch with a radius of 0.4 cm surrounded by 5 pairs of crowns. The antenna is implemented on a double-sided copper plate with an FR4-epoxy substrate of $1 \times 1\,\mathrm{cm}^2$ area and 1.6 mm thickness. This small patch operates and resonates on two frequencies 7.5 GHz and 17 GHz within C and K_u bands, respectively. The simulated and measured gains were respectively 0.8 dB and 0.2 dB at the lower frequency and 2.21 dB and 2 dB at the higher frequency. A coaxial probe feeding method is used in the simulation, and printed prototypes showed excellent consistency between measured and simulated resonance frequencies.

1. INTRODUCTION

Over the last three decades, microstrip patch antennas have become the most commonly used technology in the applications of mobile communication systems because of their light weight, low cost, low power consumption, and ease of fabrication and integration. However, in specific applications like satellite communications, there has been a demand of reducing the size of the ordinary patch antennas. For instance, mobile phones have rapidly faced a reduction in size resulting in a new evolution of patch antennas that are utilized in mobile communication to replace the traditional ones. Various techniques have been proposed by antenna designers to fulfill this reduction such as i) using metamaterial superstrate [1–3], ii) using a substrate with a relatively high permittivity [4], iii) the use of reshaping or adding slots to the patch [5, 6], iv) using fractal modification method on the ground plane [7, 8], v) using the shorting pin [9], vi) using fractal technique [10–12]. The latest, the fractal technique, shows interesting features resulting from different geometrical designs. The essential feature of the geometry in the fractal antenna aims to maximize the perimeter of the patch design so that it can transmit or receive more electromagnetic radiation within a specific area or volume. Moreover, ordinary antennas can operate at a single frequency band which means that different antennas must be used for different applications; this causes limited space problems especially for mobile applications. Fortunately, fractal antennas can operate at multi-frequency bands to overcome the limited space problem [13]. According to its geometrical configuration, fractal antennas can be divided into two main configurations: deterministic and random. Determinist objects such as Sierpinski gaskets and von Koch snowflakes have been proposed in [14, 15] to improve the efficiency and the gain. Random configuration is similar to natural phenomena, such as lightning bolts [16]. Beyond these configurations, numerous microstrip patch antennas were built according to the fractal theory to implement irregular shapes to minimize patch antennas. For instance,

Received 6 December 2021, Accepted 30 January 2022, Scheduled 8 February 2022

* Corresponding author: Jihan Salah Abdaljabar (jihan.salah@spu.edu.iq).

[1] Department of Communication Engineering, Polytechnique University, Sulaymaniyah, Iraq. [2] School of Engineering Architecture and Interior Design, Amity University, Dubai, UAE. [3] Department of Communication Engineering, Polytechnique University, Sulaymaniyah, Iraq. [4] Department of Electrical and Computer, American University of Beirut, Beirut, Lebanon.

a frequency-reconfigurable cedar-shape fractal antenna was demonstrated in 2012, and this unique small size antenna was built on a $60 \times 65\,\text{mm}^2$ substrate and resonated at 2.4 GHz as mentioned in [17]. It is interesting to notice that since 2014, antenna designers have been focusing on building microstrip patch flower antennas working on different frequency bands from 2.4 GHz to 15 GHz as illustrated in [18, 19]. Further research in this area includes the fabrication of a wheel-shape antenna in 2017 [20]. This modified wheel-shaped fractal antenna of a width of 32 mm and length of 36 mm was printed and measured to meet the demand of a small size fractal antenna.

Since February 2020, COVID-19 has spread out all around the globe; it has become a major public health pandemic that is still changing lives and daily habits. Recently, due to increasing interest in this virus, the pictures of COVID-19 have been published in most scientific and non-scientific journals. The inspiration for this antenna patch shape was taken from the silhouette of a COVID-19 virus. In February 2002, Federal Communications Commission in the United States authorized that the frequency band from 3.1 to 10 GHz can be used in the civil commercial services. This paper will adopt the design of the COVID-19 patch antenna and use the advantages of fractal geometry features to design a very small prototype suitable for dual-band wireless applications. It resonates at 7.5 GHz (in C-band) and 17 GHz (in K_u-band) which makes the proposed patch suitable for downlink of satellite communication systems, breast cancer detection, and smart home concept (at 7.5 GHz) [13, 21, 22], and it is also used in the transmission of direct broadcast services (DBS) and Fixed Satellite Service (at 17 GHz) [23]. The application of fractal geometry on the planar structure of the COVID-19 circular patch antenna results in enhancing the bandwidth of the antenna. This design is analysed using the finite element method-based software, ANSYS HFSS simulator.

2. ANTENNA CONFIGURATION AND DESIGN

The configuration of the proposed COVID-19 antenna model and the actual virus image are represented in Figure 1.

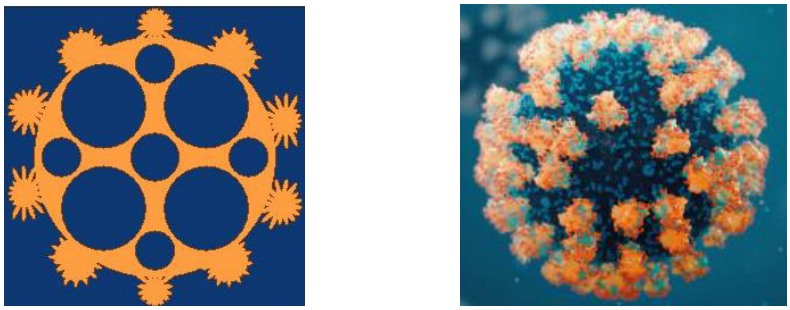

(a) (b)

Figure 1. (a) The simulated COVID-19 antenna, (b) the image of the actual virus.

The 2D and 3D simulated COVID-19 models with dimensions are shown in Figure 2. In this structure, an FR4-epoxy substrate with relative permittivity of 4.4 is used to build the microstrip patch antenna. This material has been chosen because of its availability and low cost. The overall dimensions of the substrate (L, W, h) are $(1 \times 1 \times 0.16)\,\text{cm}^3$. The main patch antenna is circular with a radius of 4 mm. The patch antenna is fed using the coaxial probe feed method, and the pin of the coaxial feed is placed at point (0 mm, −1.18 mm) with the center of the patch considered as the origin. The coaxial feed consists of three parts: the inner conductor connected to the patch with 0.735 mm radius, insulator of Teflon with a radius of 1.2 mm, and outer conductor connected to the ground with a 2.5 mm radius. This method of feeding is the best because it gives the overall patch the same shape as the COVID-19 virus shape. The main circular patch antenna is firstly built without fractals; however, the resonance frequency is extremely high because the electrical length of the antenna is low. Different fractal shapes have been demonstrated to lower the resonance frequency. The best results were optimized when nine circles were inserted. One of them is at the center of the patch of radius R_2, and four small circles of

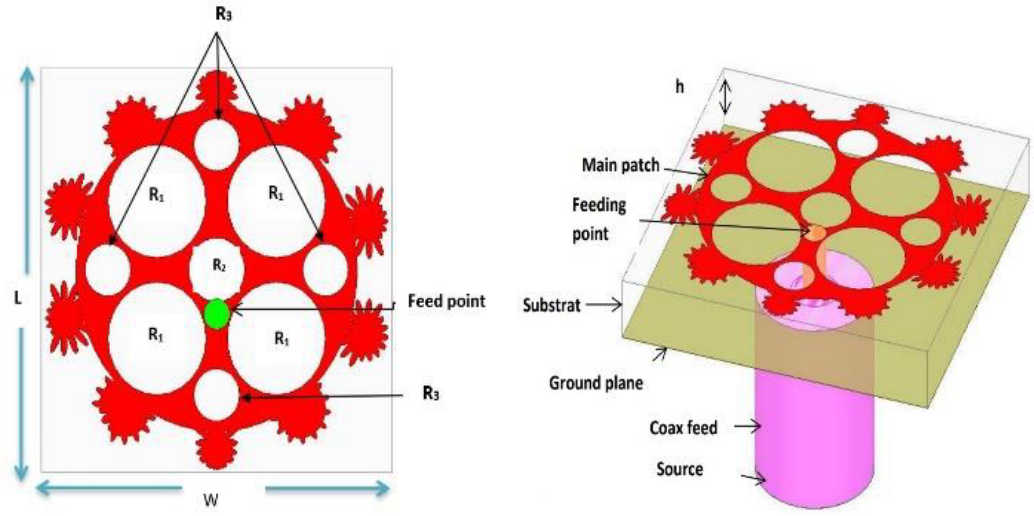

(a) (b)

Figure 2. (a) shows a two-dimensional prototype of the simulated COVID-19 patch antenna, (b) shows the three-dimensional COVID-19 patch antenna.

radius R_3 were distributed equally around the center with 90° rotation, while the other four big circles of radius R_1 were distributed equally around the center with 45° rotation. Further optimizations are done using try and error to estimate the radius of the fractal circles which give the best resonance frequency and reflection coefficient, and the final dimensions of these circles are shown in Table 1.

Table 1. Parameter descriptions of the simulated COVID-19 patch antenna.

Decryptions	Symbols	Values in (mm)
Length of the substrate	L	10
Width of the substrate	W	10
Radius of the main patch	R	4
Radius of the big fractal circle	R_1	1.4
Radius of middle fractal circle	R_2	0.8
Radius of the small fractal circle	R_3	0.65
Height of the substrate	h	1.6

The next step is drawing the crowns around the main circular patch to give it the unique shape of COVID-19 virus. Ten crowns surround the main patch with a 36° angle between adjacent crowns. The first crown on top of the main patch was initially created, and four ellipses with a major radius of 0.33 mm and a minor radius of 0.24 mm were used to make the original spike, see Figure 3(a) (Figure 3(b) is the magnified picture of Figure 3(a)). Then, two copies of this spike were rotated and duplicated around itself with angle 26° firstly (light blue color) in Figure 3(c), and −26° secondly (green color) to have 5 spikes in total, which were eventually united to make the first crown, as shown in Figure 3(d). Similarly, more spikes were added on the other pair of crowns to give each pair its unique shape similar to the original virus. This crown was rotated and duplicated with 180° to have the second crown diametrically opposite as shown in Figure 3(e). Next, by leaving a distance of 36° from the top crown, another crown with more spikes is implemented. This crown was also rotated and mirrored to have the fourth crown as shown in Figure 3(f). The same procedure is followed in Figure 3(g) and Figure 3(h), to have six and eight crowns, respectively. The final shape of the COVID-19 patch form with five pairs

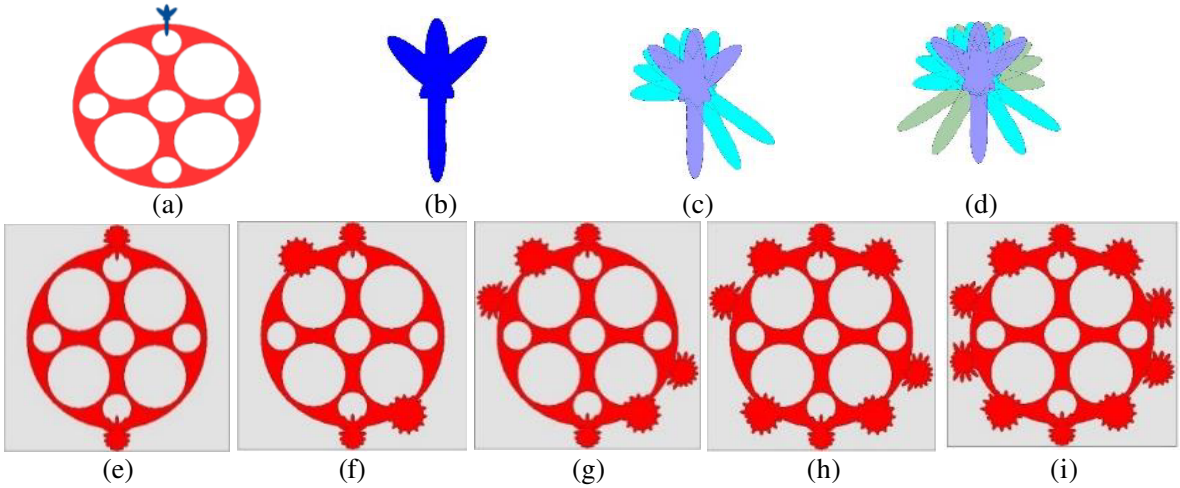

Figure 3. Steps of drawing the crowns around the main circular.

of crowns is shown in Figure 3(i).

The simulated COVID-19 patch antenna is designed with only five pairs of crowns; it is optimal to have this number of crowns depending on the results of resonance frequency and the reflection coefficient curves (S_{11}). Firstly, when the number of crowns was only 8 the antenna patch resonated at four different bands (as shown in Figure 4); unfortunately, all the four bands have narrow bandwidth, and the COVID-19 patch overall shape was unacceptable. The next step was building 12 crowns surrounding the central patch; however, the resonance frequency was completely lost. Therefore, 10 crowns were chosen to have double band frequencies with wide bandwidth, and the reflection coefficient curves at 7.5 GHz and 17 GHz are shown in Figure 4.

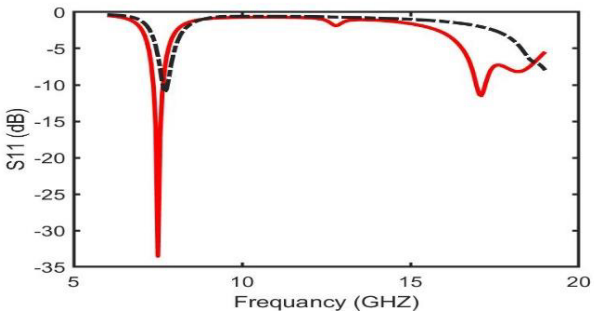

Figure 4. Simulated S_{11} curves: black line when there are 8 crowns on the antenna. Red line when there are 10 crowns on the antenna.

After optimizing the size of the substrate, the radius of the circular patch, and the number of crowns surrounding the patch, it is essential to demonstrate the fractal geometry on the main circular patch to determine the reflection coefficient and resonance frequency of the COVID-19 patch. According to Figure 5, six different images have been investigated to represent the current distribution density on the COVID-19 patch surface. Different colors are shown in Figure 5, and they represent different current distribution density values. The blue color has the least current density, and as the colors change from blue to red, the current density increases gradually until it reaches its highest value at the red color. Therefore, it is important to notice the changes in increasing the red surface area of the patch since with better current distribution (the red surface area) lower resonant frequency is obtained.

In Figure 5(a), the COVID-19 patch was designed firstly without any fractal shapes on its surface; however, the resulting current distribution density was only concentrated around the feed point. When

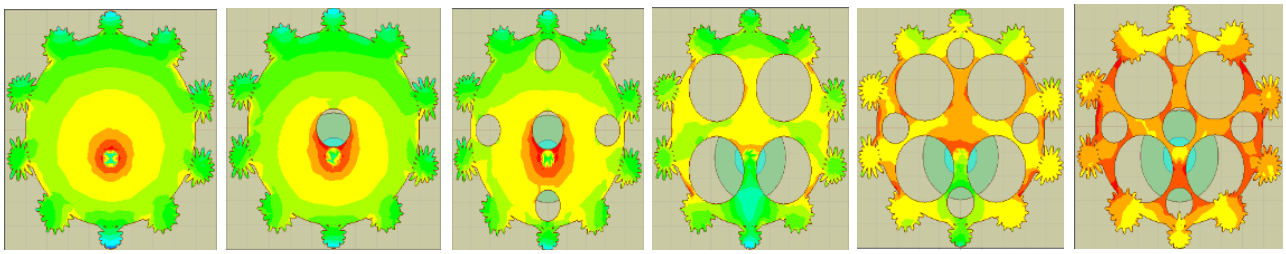

Figure 5. The current distribution density of various fractal geometries.

the first circle was iterated from the center of the patch (as shown in Figure 5(b)), the current density was distributed on a wider area far away from the feed position. In Figure 5(c), when four more circle-shaped slots were added, the current distribution density improved drastically and reached the crowns. Despite this, the resonance frequency was far from the accepted value, and when four more circles were iterated, no significant difference in the resonance frequency was detected. It was estimated to adopt a new fractal geometry as shown in Figure 5(d). The current distribution density expanded and reached the crowns, and yet the resonance frequency did not improve. Interestingly, when both of the fractal geometries of Figure 5(c) and Figure 5(d) were applied to the patch surface, the results improved dramatically. Two fractal geometries were designed, firstly the fractal geometry of Figure 5(e) and secondly the geometry of Figure 5(f). Finally, according to the current distribution density and resonance frequency results, it was decided to adopt the COVID-19 patch of Figure 5(f) as the final simulation of the COVID-19 patch shape.

3. SEMI ANALYSIS APPROACH

Before designing the patch antenna, the following equations are used to find roughly the dimensions of the circular patch antenna [24].

$$F = (8.791 \times 10^9)/(f_r\sqrt{\varepsilon_r}) \tag{1}$$

where F is the fringing factor, f_r the resonance frequency, c the free space velocity of light, and ε_r the dielectric constant. The main radius of the patch (R) is calculated as follows:

$$R = F \times \{1 + (2h/\pi\varepsilon_r F)[(\ln(\pi F/2h) + 1.7726]\}^{-1/2} \tag{2}$$

The resonance frequency corresponds to any TM_{mn0} mode is given as

$$f_{rmn0} = (c/2\sqrt{\varepsilon_r})[X_{mn}/R] \tag{3}$$

Here, n and m are modes with respect to R, and X_{mn} is the derivative of the Bessel function.

When $f_r = 7.5\,\mathrm{GHz}$, $h = 1.6\,\mathrm{mm}$, and $\varepsilon_r = 4.4$, the radius of the main patch obtained was 5.21 mm according to Equations (1) and (2). Upon doing extensive literature review, different fractal geometries were applied in order to miniaturize the antenna and increase its electrical length. It was observed that after using nine circular slots it was optimal to reduce the main radius of the patch to 4 mm, and dual frequency bands are achieved. Finally, 5 pairs of crowns are inserted to give the patch its last form of COVID-19 virus.

Adding fractal circles and crowns around the main circular patch improves both the reflection coefficient and resonance frequency. Figure 6 shows a comparison among three curves. Firstly when a simple circular patch with radius 4 mm and operating frequency 7.5 GHz was designed without crowns and fractals, it resonated at 9.9 GHz with reflection coefficient -11 dB. Secondly, when fractals were added to the main circular patch, the results further developed to become (8.8 GHz, -11.4 dB) for the lower band and (18.8 GHz, -21 dB) for the higher band. Finally, when the crowns were drawn around the fractal circular patch the resonance frequency and reflection coefficient improved dramatically to be (7.5 GHz, -37 dB) for the lower band and (17 GHz, -11.5 dB) for the higher band. From this

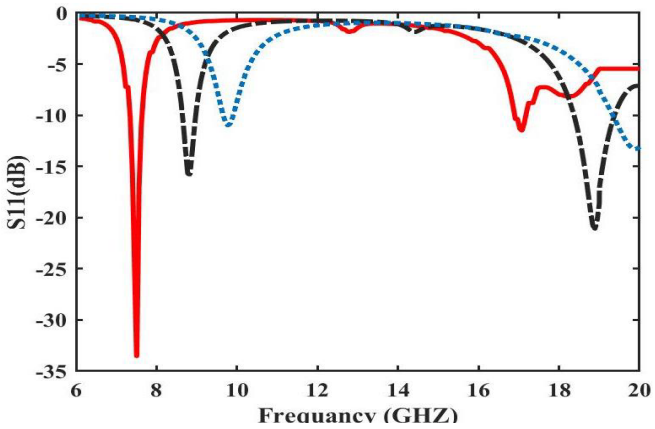

Figure 6. Blue dot line: circular patch without fractal without crowns. Black dash line: circular patch with fractals without crowns. Red solid line: circular patch with fractals with crowns.

comparison, it becomes apparent that adding the crowns around the main circular patch not only gives the patch its unique shape of the COVID-19 virus but also improves the reflection coefficient and resonance frequency of the miniature antenna.

4. RESULTS AND DISCUSSION

The three-dimensional radiation pattern was plotted, and the maximum gain was measured to be 0.8 dB at 7.5 GHz and 2.21 dB at 17 GHz as illustrated in Figure 7. Moreover, the gain and radiation efficiency are drawn concerning the frequency as shown in Figure 8.

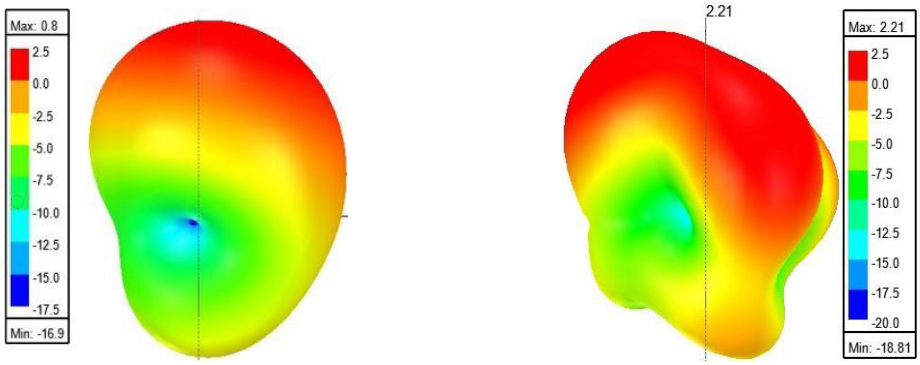

Figure 7. 3D radiation pattern of the simulated COVID-19 antenna: (a) is at 7.5 GHz and (b) is at 17 GHz.

When the COVID-19 patch antenna simulations were completed, the prototype was fabricated using FR4-epoxy substrate material and a double-sided copper plate with 1.6 mm thickness and a coaxial feed method. We have maintained a full ground in the antenna while the patch was engraved on the upper copper side. The chemical etching method was used to fabricate the patch antenna, where small details in the small spikes of the crowns surrounding the main patch were duplicated to a very accurate extent. The multi-band frequency, low weight, small size, low-cost patch antenna prototype is fabricated as shown in Figure 9. Measurements of the reflection coefficient were conducted, and results are compared to the simulated ones. The reflection coefficient versus frequency curves is plotted in Figure 10.

The radiation characteristics of the designed antenna are simulated and measured for both frequencies as shown in Figure 11. This figure presents the E and H planes for both co-polar and cross-

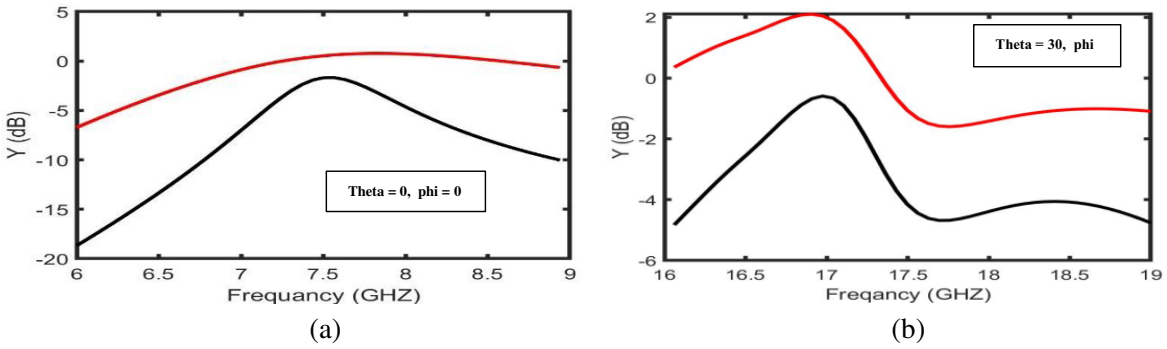

Figure 8. Simulated gain (upper red line) and radiation efficiency (lower black line) at (a) 7.5 GHz and (b) 17 GHz.

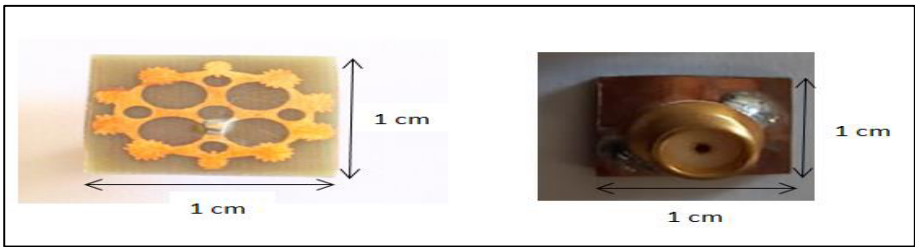

Figure 9. On left is the front view of the COVID-19 patch antenna prototype; and on right is the back view.

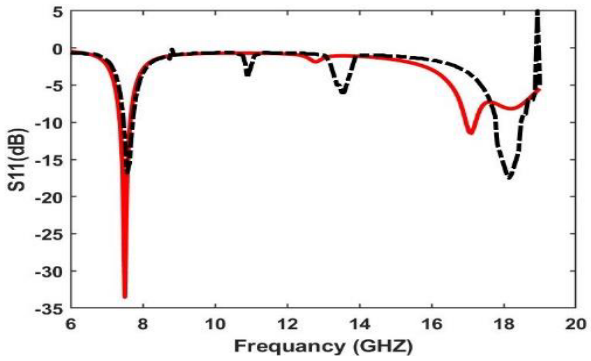

Figure 10. Comparison of the reflection coefficient of both the simulated (red solid line) and the measured (black dash line) results.

polar radiations. In the first and second images of Figure 11, the radiation patterns of the simulated and measured curves at 7.5 GHz are depicted, while in the third and fourth images, the simulated and measured radiation patterns at 17 GHz are shown. The solid line is the simulated results, and the dashed line is the measured results. The red and black lines represent the co-polar and cross-polar radiations, respectively. The co-polar and cross-polar radiations give us the polarization characteristics of the studied antenna. It is clear that the difference between the co- and cross-polar radiations is better than 30 dB for the lower band and 20 dB for the higher band in the direction of maximum radiations, and then the antenna is linearly polarized. It was found that the maximum measured gain of the designed antenna was 0.2 dB and 2 dB at frequencies of 7.5 GHz and 17 GHz, respectively.

The antenna produced is compared with other antennas with different designs, as shown in Table 3. After examining the results, we have seen that our antenna is easy to fabricate according to the layers used, and this miniature size antenna works in dual band resonance frequency.

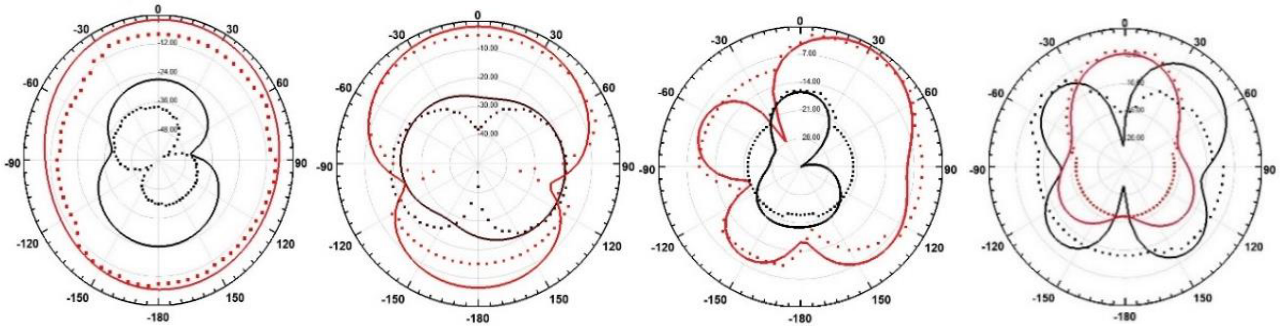

Figure 11. Radiation patterns of co-polar (red line) and cross-polar (black line) for simulated (continuous) and measured (dashed) curves at 7.5 GHz (the first and second images) and 17 GHz (the third and fourth images) respectively. Table 2 shows a comparison between the proposed work and other irregularly shaped patch antennas according to their sizes and operating band frequency.

Table 2. Comparison between COVID-19 patch antenna and other irregular shape antennas.

Reference number	**Antenna volume (cm)^3**	**Resonance frequency (GHz)**	**Gain (dB)**
[8]	69	1.28	4
[10]	17	0.193, 0.22	1.91, 2.07
[14]	24.3	1.5, 2.6	5.3, not given
[16]	6.4	2.4	2.5
[18]	5.76	3.14, 4.28, 5.1, 6.9	1.9, 10.9, 1.8, 9.3, 4
[19]	1.44	2.9, 9.5	2.8, 4.11
[20]	0.252	6	10
Proposed work	0.16	7.75, 17	0.8, 2.2

Table 3. Comparison between the proposed work and other miniaturised patch antennas.

Reference	Layers used	Patch area (mm^2)	Resonance frequency (GHz)
[21]	2	10×10	7.7
[23]	2	20×20	12.25, 14.16
[25]	3	9.5×8	15.33, 17.6
[26]	1	22×21	12.07, 14.44
[27]	1	20×20	12.38, 14.4
Proposed work	1	10×10	7.5, 17

5. CONCLUSION

The main goal of the current paper is to use the fractal geometry and the COVID-19 shape in order to create a miniature antenna for the implementation of dual-band wireless, satellite, and radar applications within C and K_u bands (when it is a part of an array) and civil commercial services. The proposed low-weight antenna operates at two different frequency bands 7.5 GHz and 17 GHz with a maximum gain of 0.8 dB and 2.21 dB respectively for the simulated and 0.5 dB and 2 dB for the measured results. This innovative patch is suitably designed so that the current distribution density reaches the far edge

of the crowns. The main purpose of these crown shapes is not only to give the patch its unique shape of COVID-19 virus but also improves the resonance frequency and reflection coefficient of the fractal circular patch. When the simulated results are finalized, the prototype is printed on a 1 cm × 1 cm substrate using chemical etching. There is an acceptable agreement between the simulated and measured results for both the input and output antenna characteristics. The discrepancy in the results is explained by errors in exact duplication of the design due to its miniature dimensions and mismatches or reflection in SMA and coaxial feed connection.

ACKNOWLEDGMENT

The authors would like to acknowledge the Lab staff at the American University of Beirut for the fabrication and testing of the antenna.

REFERENCES

1. Razi, Z. M., P. Rezaei, and A. Valizade, "A novel design of Fabry-Perot antenna using metamaterial superstrate for gain and bandwidth enhancement," *International Journal of Electronics and Communications*, 1525–1532, 2015.
2. Jahani, S., J. Rashed-Mohassel, and M. Shahabadi, "Miniaturization of circular patch antennas using MNG metamaterials," *IEEE Antennas Wirel. Propag. Lett.*, Vol. 9, 1194–1196, 2013.
3. Aziz, C. H. and A. M. Al-Hindawiia, "Electromagnetic effect of rectangular spiral metamaterial on microstrip patch antenna performance," *Journal of Modeling and Simulation of Antennas and Propagation*, Vol. 2, No. 1, 24–29, 2016.
4. Kula, J., D. Psychoudakis, W. J. Liao, C. C. Chen, J. Volakis, and J. Halloran, "Patch antenna miniaturization using recently available ceramic substrates," *IEEE Antennas Propag. Mag.*, Vol. 48, No. 6, 13–20, 2006.
5. Musselman, R. L. and J. L. Vedral, "Patch antenna size-reduction parametric study," *ACES Journal*, Vol. 34, No. 2, 288–292, February 2019,
6. Nasimuddin, Z. N. Chen, and X. Qing, "Dual-band circularly polarized S-shaped slotted patch antenna with a small frequency-ratio," *IEEE Transactions on Antennas and Propagation*, Vol. 58, No. 6, 2112–2115, June 2010.
7. Jang, H. A., D. O. Kim, and C. Y. Kim, "Size reduction of patch antenna array using CSRRs loaded ground plane," *PIERS Proceedings*, 1487–1489, Kuala Lumpur, Malaysia, March 27–30, 2012.
8. Goodwill, K., V. N. Saxena, and M. V. Kartikeyan, "Dual-band CSSRR inspired microstrip patch antenna for enhancing antenna performance and size reduction," *2013 International Conference on Signal Processing and Communication (ICSC)*, 495–497, 2013.
9. He, M., X. Ye, P. Zhou, G. Zhao, C. Zhang, and H. Sun, "A small-size dual-feed broadband circularly polarized U-slot patch antenna," *IEEE Antennas Wirel. Propag. Lett.*, Vol. 14, 898–901, 2015.
10. Dwairi, M. O., M. S. Soliman, A. A. Alahmadi, I. M. A. Sulayman, and S. H. Almalki, "Design regular fractal slot-antennas for ultra-wideband applications," *2017 Progress In Electromagnetics Research Symposium — Spring (PIERS)*, 3875–3880, St. Petersburg, Russia, May 22–25, 2017.
11. Jena, M. R., B. B. Mangaraj, and R. Pathak, "Design of a novel Sierpinski fractal antenna arrays based on circular shapes with low side lobes for 3G applications," *American Journal of Electrical and Electronic Engineering*, Vol. 2, No. 4, 137–140, 2014.
12. Chowdhury, B. B., R. De, and M. Bhowmik, "A novel design for circular patch fractal antenna for multiband applications," *2016 3rd International Conference on Signal Processing and Integrated Networks (SPIN)*, 449–453, 2016.
13. Kumar, A. and A. P. Singh, "Design of micro-machined modified Sierpinski gasket fractal antenna for satellite communications," *International Journal of RF and Microwave Computer-Aided Engineering*, Vol. 29, No. 8, e21786, 2019.

14. Prajapati, P. R., G. Murthy, A. Patnaik, and M. Kartikeyan, "Design and testing of a compact circularly polarised microstrip antenna with the fractal defected ground structure for L-band application," *IET Microw. Antennas Propag.*, Vol. 9, 1179–1185, 2015.
15. Khanna, G. and P. N. Sharma, "Fractal antenna geometries: A review," *International Journal of Computer Applications*, Vol. 153, No. 7, 29–32, November 2016.
16. Madi, M. A., M. Al-Husseini, A. H. Ramadan, M. Mervat, and A. El-Hajj, "A reconfigurable cedar-shaped microstrip antenna for wireless applications," *Progress In Electromagnetics Research C*, Vol. 25, 209–221, 2012.
17. Abraham, J., K. K. Aju John, and T. Mathew, "Microstrip antenna based on Durer pentagon fractal patch for multiband wireless applications," *International Conference on Information Communication and Embedded Systems (ICICES2014)*, 1–5, 2014.
18. Kaushal, D. and T. Shanmuganantham, "Parametric enhancement of a novel microstrip patch antenna using circular SRR loaded fractal geometry," *Alexandria Engineering Journal*, 2551–2557, 2018.
19. Gupta, M. and V. Mathur, "Wheel shaped modified fractal antenna realization for wireless communications," *International Journal of Electronics and Communications*, 257–266, 2017.
20. Bisht, N. and P. Kumar, "A dual band fractal circular microstrip patch antenna for C-band applications," *PIERS Proceedings*, 852–855, Suzhou, China, September 12–16, 2011.
21. Maria, N., M. A. Madi, and K. Y. Kabalan, "Miniaturized inward fractal antenna for breast cancer detection," *Proc. of the International Conference on Electrical, Computer and Energy Technologies (ICECET)*, December 9–10, 2021.
22. Deepak, G. and Sh. Mishr, "Smart home networkingz," *Jaipur International Journal of Converging Technologies and Management (IJCTM)*, Vol. 2, No. 2, 2016.
23. Kumar, R., G. S. Saini, and D. Singh, "Compact tri-band patch antenna for Ku band applications," *Progress In Electromagnetics Research C*, Vol. 103, 45–58, 2020.
24. Balanis, C. A., *Antenna Theory: Analysis and Design*, 3rd Edition, John Wiley and Sons Inc., New York, 2005.
25. Samsuzzaman, M., M. T. Islam, N. Misran, and M. M. Ali, "Dual band X shape microstrip patch antenna for satellite applications," *Procedia Technology*, Vol. 11, 1223–1228, 2013.
26. Vijayvergiya, P. L. and R. K. Panigrahi, "Single-layer single-patch dual band antenna for satellite applications," *IET Microw. Antennas Propag.*, Vol. 11, No. 5, 664–669, 2016.
27. Saini, G. S. and R. Kumar, "A low profile patch antenna for Ku-band applications," *International Journal of Electronics Letters*, 1–11, 2019.